DOI: 10.1002/adma.200602550

Woodpile Metallic Photonic Crystals Fabricated by Using Soft Lithography for Tailored Thermal Emission**

By *Jae-Hwang Lee*,* *Yong-Sung Kim*, *Kristen Constant*, and *Kai-Ming Ho*

3D micropatterning of materials can create advanced mechanical, chemical, or electromagnetic functionalities not observed in bulk. This is especially true for 3D periodic structures, called photonic crystals, which significantly modify optical properties of materials for light having wavelengths close to the periodicity of the patterning.[1–3] Among them, a 3D metallic photonic crystal (MPC), usually in a woodpilelike pattern,[4] has recently attracted attention because it can produce efficient thermal emitters and photovoltaic devices[5] through tailoring of the absorption spectrum.[6,7] However, its fabrication is still problematic because of challenges in 3D microfabrication at optical scales. In this letter, we report a nonphotolithographic fabrication method using soft lithography[8] and electrodeposition to produce highly layered full-metallic structures with excellent structural fidelity. By adding a homogeneous monolithic backplane to the conventional woodpile structure, the difficulty of alignment in layer-by-layer fabrication is alleviated, while preserving characteristic highly enhanced thermal radiation in a tailorable range of frequencies.

Although the tailored enhancement of absorption has been observed from woodpile MPCs fabricated by semiconductor processing,[6,7] obstacles in multilayer alignment and intricate processing still remain. As an alternative approach, direct laser writing[9,10] could be considered to create a template for woodpile MPCs. As in all approaches using a template, metal-infiltration is a critical step because of the complex 3D geometry of the template. Electrodeposition has strong potential for complete bottom-up filling rather than vapor-phase deposition, which often results in voids from blocked channels.[11,12] However, a number of requirements must be satisfied, including: complete wetting of the template, slow deposition to prevent hydrogen generation at the cathode, and good chemical and mechanical stability of the template under electrolytes. Additionally, the surface of the conducting substrate cannot have any insulating residue impeding current flow after forming the template. It is not clear whether other approaches using photolithography, including direct laser writing, are adequate for the fabrication of woodpile metallic structures using electrodeposition.

Recently, we reported a soft lithographic technique, called two-polymer microtransfer molding,[13] for the fabrication of layer-by-layer polymer microstructures using nonoptical additive processing. With this technique, a photocurable polyurethane prepolymer (J91, Summers Optical) is filled in linear microchannels of a polydimethylsiloxane-based elastomeric mold (Sylgard 184, Dow Corning) and solidified. The surface of the prefilled polymer is coated with a photocurable polymetacrylate prepolymer (SK9, Summers Optical) as an adhesive layer and the assembly is placed in contact with an indium-tin-oxide (ITO)-coated glass. Then, after curing the adhesive layer and peeling off the elastomeric mold, a layer of microrods are transferred to the ITO-coated glass. A woodpile polymer template is created after multiple transfer steps. Generally, the layer-by-layer structure requires sophisticated translational alignment to place rods of each layer in the proper position centered between the rods of alternate layers with the same orientation.

In this study, we attempted only angular alignment for the parallel arrangement of rods in different layers using a moiré-fringes-based alignment technique[14] without the translational alignment. We show here that translational alignment is not crucial in the metallic layer-by-layer structure. The multilayer polymer template was backfilled by the electrodeposition of nickel until a homogenous overlayer was formed. The overlayer served as the backplane of the photonic crystal structure and its optical contribution is discussed. The backfilling speed was slower than for a bare ITO surface, which indicates that some electrically insulating residue existed on the surface, although it was not sufficient to prohibit electroplating. The residue may have originated from the elastomer molds used in soft lithography[15] or prepolymers used in forming the polymer templates. Because of weak adhesion of the electrodeposited nickel to ITO, the backfilled structure was easily peeled off manually. The polymer template embedded in the backfilled nickel structure was chemically removed.

Figure 1 shows scanning electron microscopy (SEM) images of a free-standing 11 layer nickel structure without the backplane. The size of the fabricated nickel structures was sufficiently wide (4 mm × 4 mm) for a thermal emitter and each layer consisted of more than 1500 rods, 1.1 μm wide and

[*] Dr. J.-H. Lee, Dr. Y.-S. Kim, Prof. K.-M. Ho
Ames Laboratory-USDOE and
Department of Physics and Astronomy
Iowa State University
Ames, IA 50011 (USA)
E-mail: leejh@iastate.edu
Prof. K. Constant
Department of Materials Science and Engineering
Iowa State University
Ames, IA 50011 (USA)

[**] One of the authors (J.H.L.) thanks Prof. Johnston and E. D. Mun for the valuable discussion in temperature calibration. This work is supported by the Director for Energy Research, Office of Basic Energy Sciences. The Ames Laboratory is operated for the U.S. Department of Energy by Iowa State University under contract No. W-7405-Eng-82.

ADVANCED MATERIALS

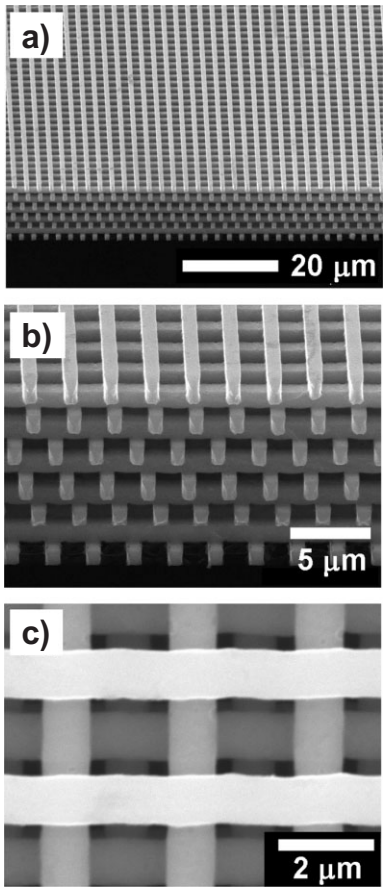

Figure 1. 3D metallic photonic crystals fabricated by using soft lithography and electrodeposition of nickel. a) Cross-sectional view of a layer-by-layer structure with 11 layers. b) Close view and c) top view of the structure.

1.2 μm high, with an in-plane rod distance of 2.6 μm. The orientation of each layer was perpendicular to the adjacent layers. To examine the structure of multidomains, each layer was intentionally misaligned, although millimeter-scale single domains were present. Therefore, we cannot classify the fabricated structure as tetragonal or face-centered-tetragonal although a local area can have a definite structure as shown in Figure 1c, for instance. However, the SEM images in Figure 1 clearly reveal complete backfilling without voids. The resulting quality is comparable to that of the metallic photonic crystal fabricated by state-of-art, costly, time-intensive semiconductor processing.[6,7]

Thermal emission from a MPC with a monolithic backplane was measured by the experimental schemes in Figure 2a with a Fourier transform IR (FTIR) spectrometer (Magna 760, Nicolet) with an ambient deuterated triglycine sulfate (DTGS) detector. Each sample was mounted on a copper block using a silver paste (597-C, Aremco) for good thermal contact and the temperature of the sample was defined as that of the copper mount. The accuracy of temperature reading was confirmed within 1 °C by the melting points of bismuth and lead. The acceptance angle and spatial resolution of the optical system were set to be 8° and 1 mm, respectively. The

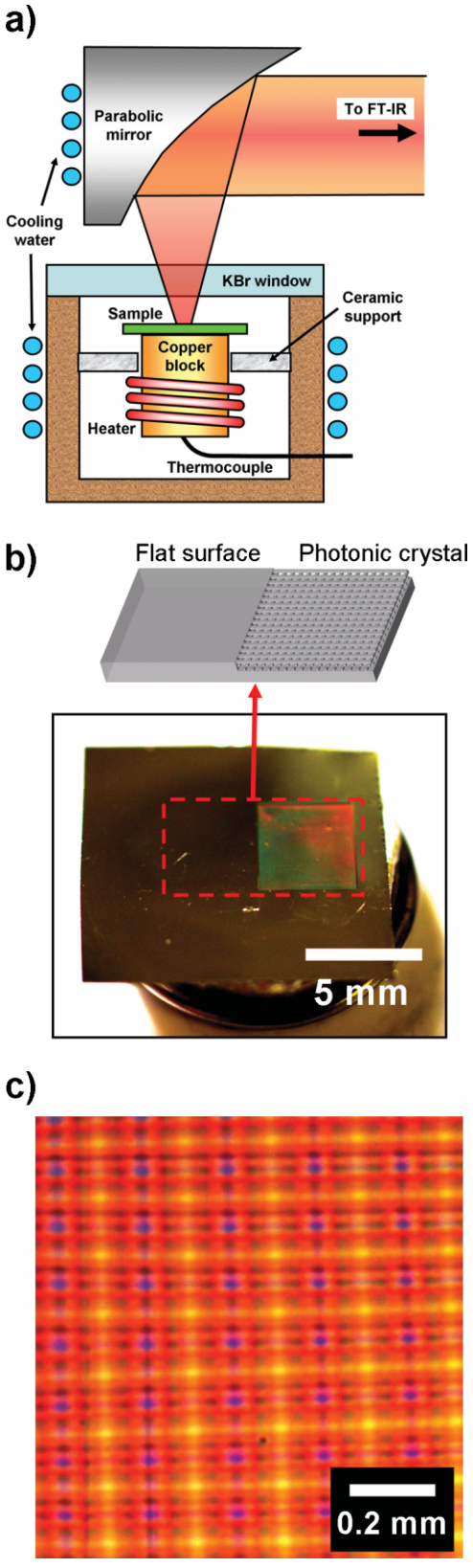

Figure 2. Measurement schemes for a photonic-crystal emitter. a) Illustration of experimental setup. b) A sample mounted on a copper block is shown with an illustration. c) Transmission moiré fringes of a four-layer polymer template.

temperatures of the vacuum chamber and optical components were held at around room temperature by cooling water and air. The measurement system was calibrated using a blackbody source, which had an emissivity higher than 0.99, at two different temperatures.[16] Because the measured thermal radiation spectrum, $L'(T,\lambda)$ (T = tempertaure, λ = wavelength), included radiation from the surroundings reflected at the sample surface, $L_0(\lambda)$, and the optical effect from the potassium bromide window in Figure 2a in the measurement of surface-normal radiation, the spectral emissivity of the sample, $\varepsilon(T,\lambda)$, can be estimated from the following approximation.

$$L'(T,\lambda) \simeq T_w\,\varepsilon(T,\lambda)\,L_{BB}(T,\lambda) + T_w^2[1-\varepsilon(T,\lambda)]L_0(\lambda) \qquad (1)$$

where L_{BB} and L_0 are the radiation powers from the blackbody at temperature T and from the surroundings, respectively, and T_w is the transmittance of the optical window. The approximation is valid because the transmittance of the sample is zero because of the homogeneous backplane and the reflection from the sample is considered as specular for the near room-temperature background radiation in which nearly all spectral power lies above the diffraction limit of the MPC (2.6 μm). Thermal-emission spectra from a patterned and a flat surface in a single sample, as seen in Figure 2b, were acquired under the same conditions for comparison. Polymer templates for more than two layers were intentionally aligned to create a multidomain MPC in order to investigate the average enhancement effect from differently aligned domains, at all possible alignments. In Figure 2c, for instance, the periodicity of moiré fringes ranged from 0.1 to 0.2 mm, which is 5 to 10 times smaller than the spatial resolution of the optical system.

Figure 3a shows the measured thermal-radiation spectra at the three different temperatures from 600 K to 800 K with corresponding blackbody-radiation spectra. The characteristic enhancement around the band edge of 3.5 μm was always observed in all of the structures, even in the single layer, and the positions of the emission peaks were pinned against the temperature change. Although a surface plasmon effect could also contribute to the enhanced absorption feature, which could appear near 2.6 μm, we presume that the major peaks of the MPCs arose from the resonance modes at the photonic band edge. For a single layer, however, the two effects seem comparable, so two peaks were observed at 2.7 μm and 3.2 μm in Figure 3b. The radiation power at the peaks approached 70 % of that of a blackbody even for a two-layer structure. According to our theoretical calculations, the substantial increase of thermal radiation of the two-layer structure was the result of the homogeneous backplane, although high emissivity was expected for at least an 8 layer structure without the backplane.[17] By integrating the radiation spectra, we can see that the total radiation power of the two-layer structure was 2.7 times smaller than that of a blackbody at 755 K (which would show the same spectral radiation power at the radiation peak wavelength of the two-layer structure). This indicates that the photonic emitter considerably reduced the required energy for a desired wavelength of light.

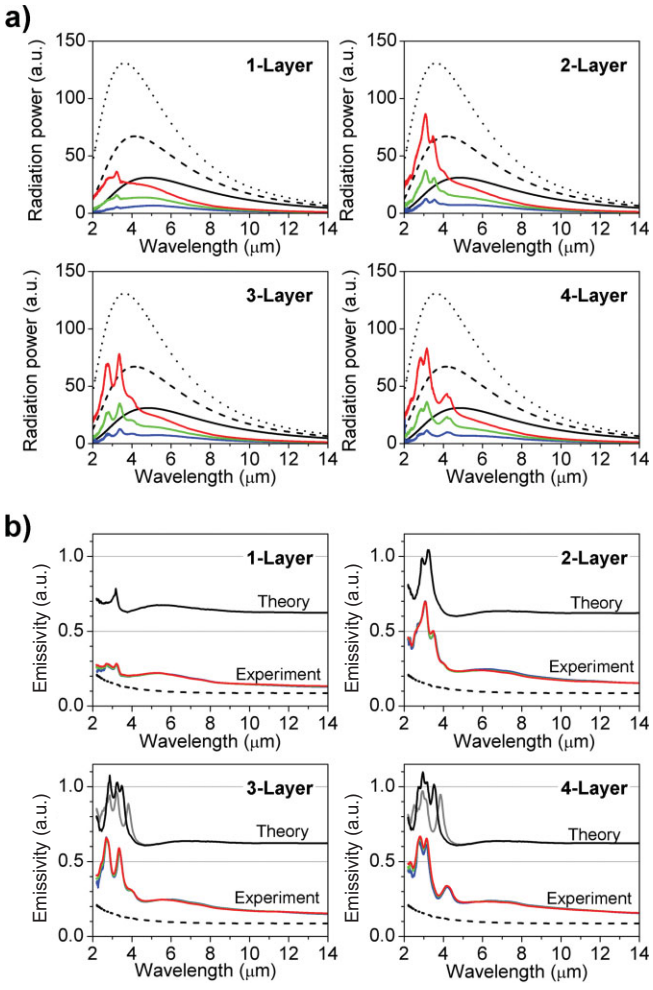

Figure 3. The radiation power and the emissivity of the MPC emitters at 600 K (blue line), 700 K (green line), and 800 K (red line). a) Thermal-radiation power from the emitters is shown as a function of the number of layers with corresponding blackbody radiation power at the three different temperatures, 600 K (solid curve), 700 K (dashed curve), and 800 K (dotted curve). b) Emissivities of each MPC emitter at different temperatures compared with the emissivity of an unpatterned surface (dashed line). The calculated emissivities of face-centered-tetragonal (black line) and tetragonal (grey line) structure are shifted by 0.5 to more easily distinguish them from the experimental values.

The emissivities of each patterned structure at different temperatures are shown in Figure 3b with the emissivity of a nonpatterned surface for comparison. All the emissivity spectra were obtained from the comparison of the radiation powers of the MPC emitter and the blackbody. The emissivity spectra were still nearly temperature-independent, consistent with a previous experimental result performed at lower temperatures,[18] and all patterned structures showed almost fivefold enhancement compared to the nonpatterned surface at the photonic-band-edge region. Metallic photonic crystals have been predicted to suppress the thermal emission in their photonic bandgap,[6,7] however, the emissivities at the wavelengths far beyond the band edge considerably exceeded those of the nonpatterned surface by roughly 50 %. This result confirms a

ADVANCED MATERIALS

previous theoretical calculation by Luo et al., which predicted excessive thermal emission in the bandgap region caused by reduced effective conductivity.[19] We notice that the performance of the two-layer MPC in Figure 3b is comparable to that of an 8-layer MPC without a backplane fabricated by a modified silicon process.[18] Because of the high rejection rate of MPCs, around 10dB/layer,[20,21] four layers were sufficient to show MPC behavior. Here, the backplane played the role of a mirror in a two-layer structure. This is an enormous advantage for an economically feasible MPC thermal emitter, as our two-layer MPC only requires a single 90° alignment.

As the number of layers increased, the number of the peaks and the enhancement range of wavelengths also increased in agreement with theoretical calculations using the analytic modal expansion method combined with a transfer-matrix technique.[22] Although the measured emissivity spectra of the three- and four-layer structure were the combined result from all of the differently aligned structures as shown in Figure 2c, the calculation only considers the three- and four-layer structures to be the two distinct structures, face-centered-tetragonal (FCT) and tetragonal. To reflect actual optical properties of the electrodeposited nickel, the refractive index and the extinction coefficients, deduced from the emissivity spectrum of nonpatterned nickel using Kramers–Kronig analysis[23] and Kirchoff's law, were used for the calculations. All calculated angle-dependent emission spectra in the acceptance angle were averaged with the weighting factors given by Lambert's cosine law.[24] Overall characteristics of the MPCs were in agreement with the calculations, although the measured emissivities were larger than the calculations. The discrepancy may arise from the surface roughness of individual bars in the MPCs. The existence of clear peaks in the emissivity of three- and four-layer MPCs confirms that the peaks are common for all differently aligned structures, which is also seen in the calculation data.

The basic fabrication method presented here is a powerful tool for creating highly layered metallic microstructures with excellent structural fidelity for various photonics applications. Additionally, it is low-cost and tailorable. By introducing a homogeneous backplane to the conventional woodpile structure, significant selective enhancement in thermal radiation is achieved from a two-layer structure requiring only coarse perpendicular alignment. This backplane also provides mechanical reinforcement to improve the durability of the structure. Furthermore, we have demonstrated that unaligned three- or four-layer structures can be useful for tuning the characteristics of thermal radiation because of the existence of universal peaks in the unaligned structures.

Experimental

The commercially available electrodeposition electrolyte kit (Bright nickel, Caswell) was used without modification for the electrodeposition of nickel. An ITO-coated substrate (8–12 Ω, SPI Supplies) was sonicated in a water-based detergent for an hour and thoroughly rinsed with distilled water. After fabrication of the polymer template [13] on the ITO substrate, the template was submerged into the electrolyte in a chamber and the surrounding pressure was subsequently reduced to a level where the electrolyte started to boil at room temperature and then recovered to atmospheric pressure. After 10 cycles of depressurization, we observed that the polymer template wetted completely within 10 min. The pressure cycling had two effects: first, volume expansion of the captured air in the template; second, depletion of dissolved air in the electrolyte because of lower gas solubility at lower pressure. After wetting occurred, the electrodeposition was performed at room temperature with a current density 0.15 mA mm^{-2} until a thick homogeneous layer over the template was formed. Required deposition time for a 40 μm thick homogeneous layer was approximately two to four hours depending on the number of layers. The electrolyte was continuously stirred and filtered during the electrodeposition. The backfilled template was peeled off manually and cleaned with distilled water. The polymer template was removed by submerging it in a 30 wt % aqueous solution of potassium hydroxide for 10 min at room temperature. The MPC was rinsed in distilled water and dried with pressurized nitrogen following the polymer removal. As the potassium hydroxide solution etched only the polyurethane (J91), the bonding material (SK9) remained after etching. However, there was no noticeable effect from the residue of SK9 because of its small amount and thermal decomposition at high temperature.

Received: November 10, 2006
Revised: January 19, 2007
Published online: February 19, 2007

[1] E. Yablonovitch, *Phys. Rev. Lett.* **1987**, *58*, 2059.
[2] S. John, *Phys. Rev. Lett.* **1987**, *58*, 2486.
[3] K.-M. Ho, C. T. Chan, C. M. Soukoulis, *Phys. Rev. Lett.* **1990**, *65*, 3152.
[4] K.-M. Ho, C. T. Chan, C. M. Soukoulis, R. Biswas, M. Sigalas, *Solid State Commun.* **1994**, *89*, 413.
[5] S. Y. Lin, J. Moreno, J. G. Fleming, *Appl. Phys. Lett.* **2003**, *83*, 380.
[6] S. Y. Lin, J. G. Fleming, I. El-Kady, *Appl. Phys. Lett.* **2003**, *83*, 593.
[7] J. G. Fleming, S. Y. Lin, I. El-Kady, R. Biswas, K.-M. Ho, *Nature* **2002**, *417*, 52.
[8] Y. Xia, G. M. Whitesides, *Annu. Rev. Mater. Sci.* **1998**, *28*, 153.
[9] H.-B. Sun, S. Matsuo, H. Misawa, *Appl. Phys. Lett.* **1999**, *74*, 786.
[10] M. Deubel, G. von Freymann, M. Wegener, S. Pereira, K. Bush, C. M. Soukoulis, *Nat. Mater.* **2004**, *3*, 444.
[11] L. Xu, W. L. Zhou, C. Frommen, R. H. Baughman, A. A. Zakhidov, L. Malkinski, J.-Q. Wang, J. B. Wiley, *Chem. Commun.* **2000**, 997.
[12] C. Cuisin, A. Chelnokov, J.-M. Lourtioz, D. Decanini, Y. Chen, *J. Vac. Sci. Technol. B* **2000**, *18*, 3505.
[13] J.-H. Lee, C.-H. Kim, K.-M. Ho, K. Constant, *Adv. Mater.* **2005**, *17*, 2481.
[14] J.-H. Lee, C.-H. Kim, Y.-S. Kim, K.-M. Ho, K. Constant, W. Leung, C.-H. Oh, *Appl. Phys. Lett.* **2005**, *86*, 204 101.
[15] J. N. Lee, C. Park, G. M. Whitesides, *Anal. Chem.* **2003**, *75*, 6544.
[16] J. Ishii, A. Ono, *Meas. Sci. Technol.* **2001**, *12*, 2103.
[17] S. Y. Lin, J. G. Fleming, Z. Y. Li, I. El-Kady, R. Biswas, K.-M. Ho, *J. Opt. Soc. Am. B* **2003**, *20*, 1538.
[18] C. H. Seager, M. B. Sinclair, J. G. Fleming, *Appl. Phys. Lett.* **2005**, *86*, 244 105.
[19] C. Luo, A. Narayanaswamy, G. Chen, J. D. Joannopoulos, *Phys. Rev. Lett.* **2004**, *93*, 213 905.
[20] E. Özbay, B. Temelkuran, M. Sigalas, G. Tuttle, C. M. Soukoulis, K. M. Ho, *Appl. Phys. Lett.* **1996**, *69*, 3797.
[21] J.-H. Lee, C.-H. Kim, Y.-S. Kim, K.-M. Ho, K. Constant, C. H. Oh, *Appl. Phys. Lett.* **2006**, *88*, 181 112.
[22] Z.-Y. Li, K.-M. Ho, *Phys. Rev. B: Condens. Matter Mater. Phys.* **2003**, *67*, 165 104.
[23] S. S. Mitra, in *Handbook of Optical Constants of Solid* (Ed: E. D. Palik), Academic, London **1985**, Ch. 11.
[24] M. Born, E. Wolf, *Principles of Optics*, Pergamon, Oxford **1989**, Ch 4.

